The effect of strain amount on corrosion behavior of EDDQ steel sheet

Vplyv stupňa deformácie na korózne vlastnosti hlbokoťažného oceľového plechu

Brezinová J., Slota J., Tomáš M., Koncz J.
TU Košice
E-mail: janette.brezinova@tuke.sk

This paper presents the results of research aimed to measuring the corrosion properties of EDDQ steel sheet. The strain amount influence to the corrosion properties of the steel sheet for drawn parts has been proven by the modern methods of corrosion monitoring such as Electrochemical Impedance Spectroscopy. Corrosion rate was assessed using electrochemical methods in 0.1 M solution of NaCl. Experimental studies have pointed out if strain amount increases the corrosion rate of the steel sheet increases too.

Príspevok prezentuje výsledky výskumu získané meraním koróznych vlastností hlbokoťažnej ocele. Vplyv stupňa deformácie na korózne vlastnosti oceľového plechu pre hlboké ťahanie bol identifikovaný modernými metódami monitoringu korózie, ako je elektrochemická impedančná spektroskopia. Korózna rýchlosť bola hodnotená pomocou elektrochemickej metódy v 0.1 M roztoku NaCl. Výsledky experimentov ukázali, že zvyšovaním stupňa deformácie sa korózna rýchlosť oceľového hlbokoťažného plechu tiež zvyšuje.

INTRODUCTION

Recent trends in the manufacture of car bodies are aimed at using advanced high strength and ultra-high strength steels. These steels reach to high level of mechanical properties. Elimination of steel body weight using advanced materials is one of the major trends in the design of cars. In the manufacture of cars are used coated body sheets which are subjected to acid rain, temperature differences, sunlight, oxygen, road salt etc. throughout their lifetime. Therefore, corrosion protection is a very important part of the car production process. Body sheet metal used for making car body are normally zinc galvanized or modified in other ways (e.g. by cataphoresis). The zinc is non-noble metal with tendency to passivation. When it is contacted with the steel, it behaves as anode and suppresses activity of the steel, which is base for the corrosion protection of metallic materials [1-4]. Protective zinc coating has to provide higher resistance of the whole protective system against perforation corrosion of body sheets. Another function of Zn coating is the longest corrosion protection in cavities and crevices where the coating system is poor or incomplete. Automobile steel sheets are hot dip galvanized or electrogalvanized. Zn coating may be single or double sided. Zinc-coated car body sheets show high corrosion resistance. During deformation seizing of zinc coating, failure of cohesion between Zn coatings and the substrate or exposures of the base material surface often occur. In car body sheets it is necessary to monitor the deformation process itself and the effect of deformation on the zinc coat [5, 6]. The important thing is to find out how the degree of deformation affects the corrosion characteristics of Zn coating (the current density, corrosion potential, corrosion rate and polarization resistance). The presented contribution aims at determination the effect of car body steel sheet deformation on change the corrosive properties of the applied coating using an Electrochemical Impedance Spectroscopy [7, 8].

EXPERIMENTAL PROCEDURE

Test samples for experimental research have been supplied in a state after deformation of the cold rolled steel sheet DC 06 (EN 10130). Chemical composition of the base material is shown in Table 1 and mechanical properties are in Table 2.

Tab. 1. Chemical composition of base material DC06 in % by weight / *Chemické zloženie základného materiálu DC06 v hm.%*

C	Mn	P	S	Ti
0.020	0.250	0.020	0.020	0.300

Tab. 2. Mechanical properties of base material DC06 / *Mechanické vlastnosti základného materiálu DC06*

$R_{p0,2}$ (MPa)	R_m (MPa)	A_{80} (%)	r_m (-)	n_m (-)
148	293	48.9	1.753	0.258

The base material was coated by double-side zinc ZE 75/75, coating weight of 54 g/m². Before biaxial deep drawing, the deformation grid of points 0.5 mm in diameter and 1 mm in horizontal and vertical distance was electrolytically etched on the surface for 3D optical photogrammetric measurement of drawn part's deformation. Subsequently, the deep drawing test with biaxial stress state was carried out on the test device Erichsen 145-60 using Nakajima tool. Test samples for measurement of corrosion properties have been taken from the four areas of drawn part: sample No. 1 – undeformed material, sample No. 2 – material with localised deformation, sample No. 3 – material above the fracture AND sample No. 4 – material from the highest point of the drawn part.

Thinning of the steel sheet was measured by 3D optical photogrammetric system ARGUS. Corrosion resistance of samples was determined by Electrochemical Impedance Spectroscopy using measurement device SP 150 Bio-Logic and software EC-Lab V10. The device can measure electrochemical parameters in different extent. Tafel analysis allows to determine corrosion current i_{corr} (and also corrosion current density I_{corr}) and corrosion potential E_{corr}. The polarization resistance R_p was determined by EIS as well. Measurement of electrochemical parameters was performed in 0.1 M solution of NaCl. Reference electrode was saturated calomel electrode, working electrode was test sample and auxiliary electrode was platinum electrode. Parameters used for the potentiodynamic tests were as follows: stabilization time was 600 s; the polarization of the sample was performed in the range from -150 mV from the free corrosion potential to +1000 mV against the reference electrode; the rate of corrosion potential was 1 mV/s; the surface area was 0,636 cm². The frequency change for the EIS varied from 100 kHz to 1mHz with 10 points per decade, and the width of the sinusoidal voltage signal applied to the system was 5 mV.

For test samples No. 1, 3 and 4 an equivalent measuring circuit for the intact coating surface with a constant phase shift has been used as it is shown in Fig. 1, where R1 is the resistance of the electrolyte, R2 = Rp is the polarization resistance and Q2 is a constant phase element. For the sample No. 2 from the material with localised deformation an equivalent measuring circuit for the damaged coating surface with a constant phase shift has been used. The measuring circuit has been extended by R3 parameter representing the polarization resistance near the failure, constant phase elements Q1 representing the capacity of corrosion products, double layer Q3 and the resistance of electrolyte in the pores R2, Fig. 2.

RESULTS

Thickness of the steel sheet after deformation by biaxial stretching has been measured by photogrammetric system ARGUS. From the major strain (Fig. 3) and minor strain (Fig. 4) were calculated changes of thickness on the bulged sample. The thinning of steel sheet is shown in Fig. 5 in color scale. The thickness change distribution on bulged hemisphere depending on the developed length of the drawn part is shown in Fig. 6.

Thinning of the steel sheet after biaxial stretching shown in Fig. 5 is expressed as a percentage of initial steel sheet thickness 0.87 mm. For sample No. 1 taken from the hemisphere bottom thickness of the material hasn't changed. The maximum thinning of 40 % has been measured on the perimeter of crack where sample No. 2 has been taken. The sample No. 3 has been taken approx. 7 mm from the sample No. 2 and the thinning of 34 ± 2 % has been measured. The sample No. 4 has been taken at the top of the hemisphere where thinning of 17 ± 2 % has been measured.
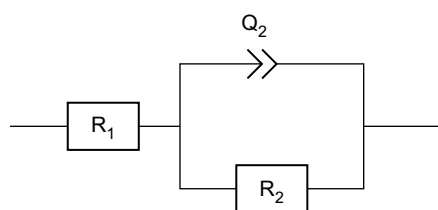

Fig. 1. Equivalent circuit for intact coating
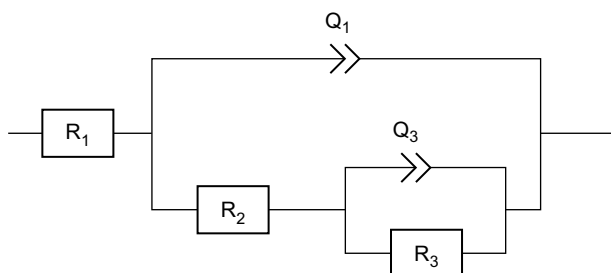*Obr. 1. Ekvivalentný obvod pre neporušený povlak*

Fig. 2. Equivalent circuit for damaged coating
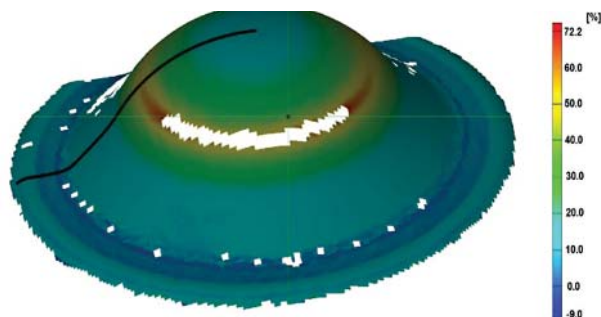*Obr. 2. Ekvivalentný obvod pre porušený povlak*

Fig. 3. Distribution of major strain on bulged sample of EDDQ steel sheet
Obr. 3. Rozloženie hlavnej deformácie na vzorke z hlbokoťažnej ocele (EDDQ) po dvojosovom vypínaní

Fig. 7 and Fig. 8 show corrosion potential E_{corr} and corrosion current density I_{corr} of samples measured by Tafel analysis. The lowest value I_{corr} was found in undeformed material – sample No. 1, the highest value has been found in area of material fracture – sample No. 2, where the highest thinning of 40 % was achieved.
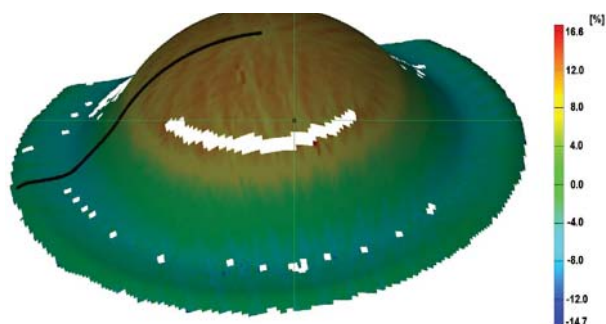

Fig. 4. Distribution of minor strain on bulged sample of EDDQ steel sheet
Obr. 4. Rozloženie vedľajšej deformácie na vzorke z hlboko-ťažnej ocele (EDDQ) po dvojosovom vypínaní
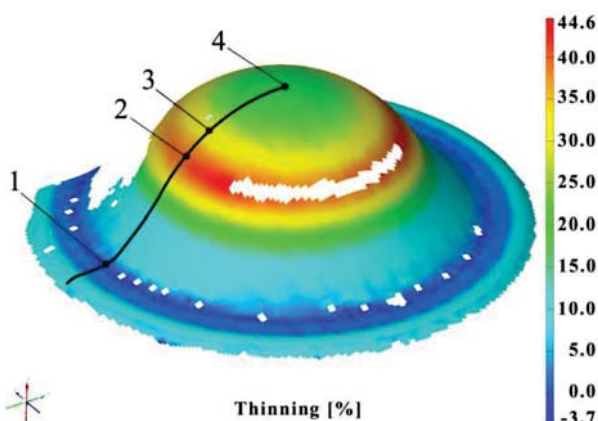

Fig. 5. Thinning of EDDQ sheet after biaxialstretching
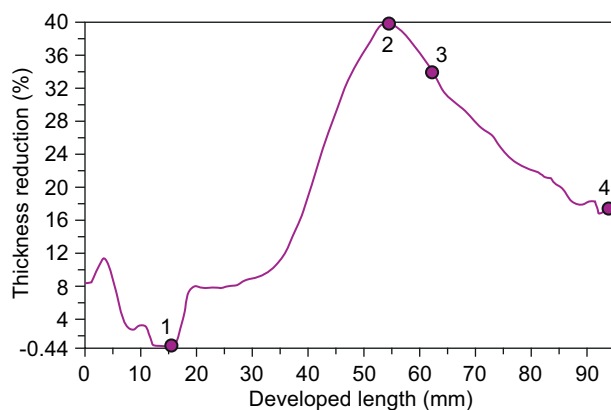*Obr. 5. Stenčenie EDDQ ocele po dvojosovom vypínaní*

Fig. 6. Change of the material thickness after biaxial stretching
Obr. 6. Zmena hrúbky materiálu po dvojosovom vypínaní

Polarization resistance R_p has been measured by EIS with values: 25 kΩ for sample No. 1 – undeformed base material; 1.25 kΩ for sample No. 2 – maximum deformation; 2.94 kΩ for sample No. 3 – above the fracture; 5.66 kΩ sample No. 4 – top of the dome. The lowest polarization resistance of 1.25 kΩ as well as the highest current density i_{corr} of 16 μA were found for sample No. 2 in the area of maximum deformation of the material. Thus, the higher probability of corrosion processes initiation is supposed. Experimentally measured results showed that the deformation of the material has a significant influence on the corrosion resistance of coatings applied.
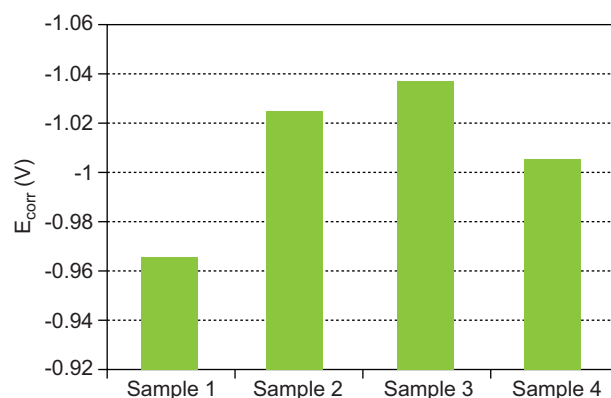

Fig. 7. Corrosion potential of Zn coating in measured areas
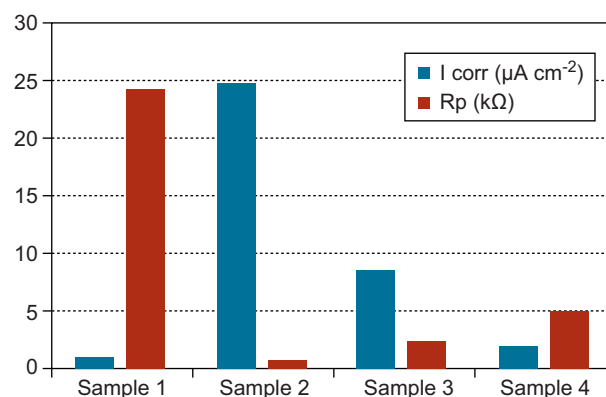*Obr. 7. Korózny potenciál Zn povlaku v meraných oblastiach*

Fig. 8. Corrosion current density of Zn coating in measured areas
Obr. 8. Korózna prúdová hustota Zn povlaku v meraných oblastiach

The results of electrochemical impedance spectroscopy (Nyquist plots) are in Fig. 9. Figure 10 shows the potentiodynamic curves of the four exposed samples. The measurement locations (sample 1-4) are identical to those of Fig. 5. The fastest dissolution of the coating took place on the undamaged sample (sample 1) up to potential -0.9 V. After this value a very compact zinc oxide layer was created on the surface and the corrosion current

growth was slowed down. Despite rapid corrosion the current of sample 1 was the lowest. Anodic part of the potentiodynamic curve (sample 4) can be divided into three areas. The first between E_{corr} and potential -0.93 with slow increase of i_{corr} due to formation a thin film of corrosion products. The second area between -0.93 V and -0.89 V with a sharp increase of i_{corr} due to localized corrosion (damaged layer of corrosion products). Anodic part of the curve is very similar to the curve of the sample 3.
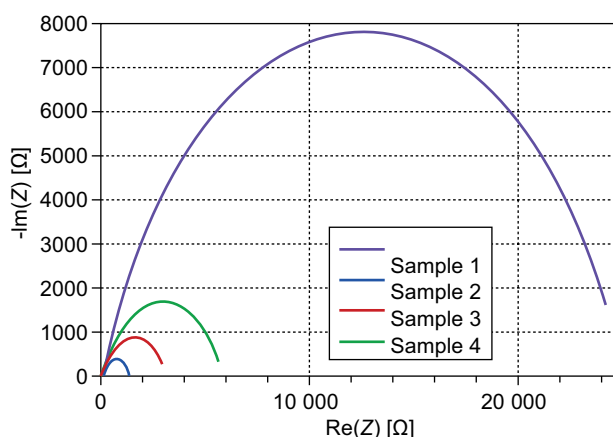

Fig. 9. Electrochemical impedance spectroscopy of EDDQ steel sheet
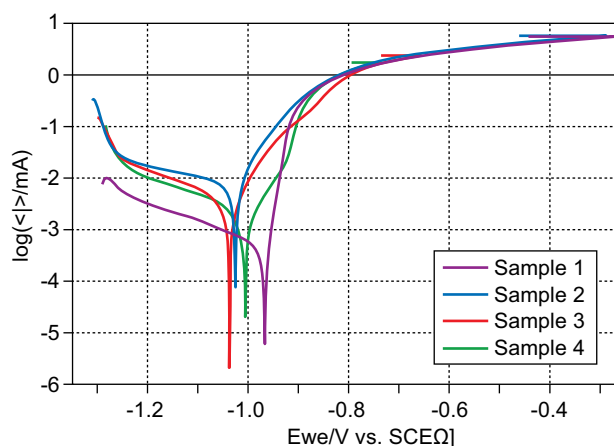*Obr. 9. Elektrochemická impedančná spektroskopia oceľového hlbokoťažného plechu*

Fig. 10. Potentiodynamic curves of the four exposed samples
Obr. 10. Potenciodynamické krivky štyroch skúšaných vzoriek

CONCLUSIONS

Based on Tafel analysis of samples with different deformation degree, specified by the thinning of steel sheet, the corrosion potential value E_{corr} and the corrosion current density value I_{corr} have been determined. The results have pointed out the corrosion rate is affected mainly by the degree of deformation. Increasing the deformation degree has led to increasing the corrosion rate of zinc coating as well. Electrochemical impedance spectroscopy allowed finding out polarization resistance R_p. The highest polarization resistance was found in undeformed material, the lowest in the region of material fracture. The knowledge is consistent with the measured values of the corrosion current density. Experimental results point to the fact that the corrosion resistance of zinc coating is significantly affected by the degree of deformation.

Acknowledgements

REFERENCES

1. Vratna, J., et al., Room temperature corrosion properties of AZ31 magnesium alloy processed by extrusion and equal channel angular pressing. *J. Mater. Sci.* **2013**, 48, 4510-4516.
2. Bukovinova, L., Hadzima, B., Electrochemical characteristics of magnesium alloy AZ31 in Hank's solution. *Corros. Eng. Sci. Technol.* **2012**, 47, 352-357.
3. Jafari, H., et al., EIS study of corrosion behavior of metallic materials in ethanol blended gasoline containing water as a contaminant, *Fuel* **2011**, 90**,** 1181-1187.
4. Mouanga, M., Puiggali, M., Devos, O., EIS and LEIS investigation of aging low carbon steel with Zn–Ni coating, *Electrochim. Acta* **2013**, 106, 82-90.
5. Frącz, W., Stachowicz, F., Pieja, T., Aspects of verification and optimization of sheet metal numerical simulations process using the photogrammetric system, *Acta Metall. Slovaca* **2013**, 19**,** 51-59.
6. Slota, J, et al., The sensitivity of a photogram. method in formability analysis, *Acta Mechanica et Automatica* **2013**, 7, 117-123.
7. Barranco, V., Feliu Jr. S., Feliu, S., EIS study of the corrosion behaviour of zinc-based coatings on steel in quiescent 3% NaCl solution. Part 1: directly exposed coatings, *Corros. Sci.* **2004**, 46, 2203-2220.
8. Walkner, S., Hassel, A.W., Combined chemical and EIS study of the reaction of zinc coatings under alkaline conditions, *Electrochim. Acta* **2014**, 131, 130-136.